

### **IISE Transactions**



ISSN: 2472-5854 (Print) 2472-5862 (Online) Journal homepage: http://www.tandfonline.com/loi/uiie21

# Scale-up modeling for manufacturing nanoparticles using microfluidic T-junction

Yanqing Duanmu, Carson T. Riche, Malancha Gupta, Noah Malmstadt & Qiang Huang

To cite this article: Yanqing Duanmu, Carson T. Riche, Malancha Gupta, Noah Malmstadt & Qiang Huang (2018): Scale-up modeling for manufacturing nanoparticles using microfluidic T-junction, IISE Transactions, DOI: 10.1080/24725854.2018.1443529

To link to this article: <a href="https://doi.org/10.1080/24725854.2018.1443529">https://doi.org/10.1080/24725854.2018.1443529</a>







### Scale-up modeling for manufacturing nanoparticles using microfluidic T-junction

Yanqing Duanmu, Carson T. Riche, Malancha Gupta, Noah Malmstadt and Qiang Huang

Viterbi School of Engineering, University of Southern California, Los Angeles, CA, USA

### **ABSTRACT**

Nanoparticles have great potential to revolutionize industry and improve our lives in various fields such as energy, security, medicine, food, and environmental science. Droplet-based microfluidic reactors serve as an important tool to facilitate monodisperse nanoparticles with a high yield. Depending on process settings, droplet formation in a typical microfluidic T-junction is explained by different mechanisms, squeezing, dripping, or squeezing-to-dripping. Therefore, the manufacturing process can potentially operate under multiple physical domains due to uncertainties. Although mechanistic models have been developed for individual domains, a modeling approach for the scale-up manufacturing of droplet formation across multiple domains does not exist. Establishing an integrated and scalable droplet formation model, which is vital for scaling up microfluidic reactors for large-scale production, faces two critical challenges: the high dimensionality of the modeling space; and ambiguity among the boundaries of physical domains. This work establishes a novel and generic formulation for the scale-up of multiple-domain manufacturing processes and provides a scalable modeling approach for the quality control of products, which enables and supports the scale-up of manufacturing processes that can potentially operate under multiple physical domains due to uncertainties.

#### **ARTICLE HISTORY**

Received 8 November 2016 Accepted 10 February 2018

#### **KEYWORDS**

Scale-up modeling; nanomanufacturing; quality engineering

### 1. Introduction

Synthesis of solid particles, liquid droplets, and gas bubbles is critical for pharmaceutical and chemical engineering applications (Demello, 2006; Wang, Jiao, Huang, Yang, and Nguyen, 2009; Xu et al., 2009). Droplet-based microfluidic devices manipulate immiscible fluids in channels of micrometer size (Thorsen et al., 2001; Anna et al., 2003; Link et al., 2004; Garstecki et al., 2006; Christopher and Anna, 2007; Christopher et al., 2008; Fu et al., 2009; Tan et al., 2009; Zhao and Middelberg, 2011). The high surface-area-to-volume ratio within microchannels guarantees a uniform temperature throughout the reaction volume, and convective mixing within droplets ensures rapid homogenization. These properties make droplet microfluidic reactors a viable technology for the scalable synthesis of high-quality metal nanoparticles.

In order to produce particles on an industrial scale with low cost, microfluidic reactors need to be scaled up for high throughput and high yield with tight control over droplet size (Christopher *et al.*, 2008; Teh *et al.*, 2008; Lazarus *et al.*, 2012; Riche *et al.*, 2014). Scale-up modeling, which refers to the process modeling approaches that enable and support economical production at commercial scale, is thus crucial for the quality control of nanoparticles (Xu *et al.*, 2015). Scale-up modeling of the droplet formation in the microfluidic channels face several key challenges:

1. *High dimensionality*. Description of droplet formation in microfluidic channel involves a large number of physical parameters or quantities. Even by conducting dimensional analysis using a scaling law (Garstecki *et al.*, 2006; De Menech *et al.*, 2008; Glawdel and Ren, 2012), the

number of obtained dimensionless numbers can be large, which gives rise to a high-dimensional problem. For instance, droplet size after scaling is proposed to be a function of more than five dimensionless numbers in the squeezing-to-dripping domain with each being a combination of multiple physical parameters (Gupta and Kumar, 2010; Glawdel and Ren, 2012). This poses both experimental and modeling challenges to understand the response surface in a high-dimensional space. Currently, the droplet formation experiment in practice uses the one-factor-at-a-time approach, i.e., testing one dimensionless number at a time and fixing the rest (Garstecki et al., 2006; Christopher et al., 2008; De Menech et al., 2008; Xu et al., 2008; Wang, Lu, Xu, and Luo, 2009; Zhang and Wang, 2009; Fu et al., 2010; MaGlawdel and Ren, 2012), which only guarantees the understanding in a projected low-dimensional space.

2. Multiple physical domains. The droplet formation in a microfluidic channel is a multiple-domain (Christopher et al., 2008; Xu et al., 2008; Wang, Lu, Xu, and Luo, 2009; Zhang and Wang, 2009; Fu et al., 2010), and a microfluidic T-junction can produce droplets either in squeezing, dripping, or squeezing-to-dripping domain (due to our focus on producing monodisperse droplets, a jetting domain is not herein discussed). Since different domains are dominated by different mechanisms, model structures depicting droplet formation vary with physical domains, which significantly increases the complexity in experimentation and modeling. Current practice is to discover individual domains through

experimentation and then establish individual models within each domain. For instance, the domains are classified based on the capillary number Ca: squeezing with Ca < 0.002, squeezing-to-dripping with 0.002 < Ca < 0.01, dripping with 0.01 < Ca < 0.3, and jetting domain with Ca > 0.3 (Xu  $et\ al.$ , 2008). In the squeezing domain, the droplet formation process is explained by the pressure drop across the droplet during formation; whereas in the dripping domain, the process is interpreted by the balance between shear force and interfacial force. However, there are inconsistencies and ambiguity in defining the boundaries of physical domains (De Menech  $et\ al.$ , 2008), which hinders the application of these models in full-scale manufacturing.

To address these challenges for full-scale production, this work aims at establishing a unified scale-up model across multiple domains under uncertainties. In the rest of this article, Section 2 introduces our model formulation and methodology for the multiple-domain scale-up modeling problem. Section 3 applies and demonstrates the proposed generic formulation and methodology to predict droplet formation in the coated microfluidic T-junction, with discussions in Section 4. We conclude in Section 5.

### 2. Scalable modeling methodology for multiple-domain manufacturing process

In order to scale-up manufacturing processes, we need to first address the so-called scale-up issue: how to translate the understanding of a process from lab scale to commercial scale such that the optimal properties can be determined *a priori* for future operations. The science base to achieving the scalability of engineering models is the scaling law, which captures the scale-invariant characteristics of an engineering system (Barenblatt, 2003; Zlokarnik, 1991). Dimensional analysis serves as an important tool to transform the parameter space to the so-called  $\Pi$ -space spanned by dimensionless numbers, which achieves dimension reduction and ensures the scalability of models. Note that although there is no unique selection of dimensionless numbers, the dimension of  $\Pi$ -space is uniquely determined by dimensional analysis.

Droplet formation in microfluidic channels represents a class of "multiple-domain" scale-up modeling problems, which involve different physical phenomena and mechanisms (Huang et al., 2011; Wang et al., 2013). Since the boundaries between different physical domains can sometimes be ambiguous, the physical domain to which the process belongs is often not known often not known a priori. Our objective is to establish a unified scale-up model across multiple domains under uncertainties to facilitate full-scale production. Our methodology is illustrated in Figure 1. We first conduct dimensional analysis to formulate the problem in the  $\Pi$ -space. Then, we identify the primary factor and secondary factor for further dimension reduction.

**Definition 1.** The primary factor consists of dimensionless numbers that characterize the physical domains of engineering systems; the rest of the dimensionless numbers form the secondary factor. Each physical mechanism, which is likely to dominate a certain domain, is then characterized by a model

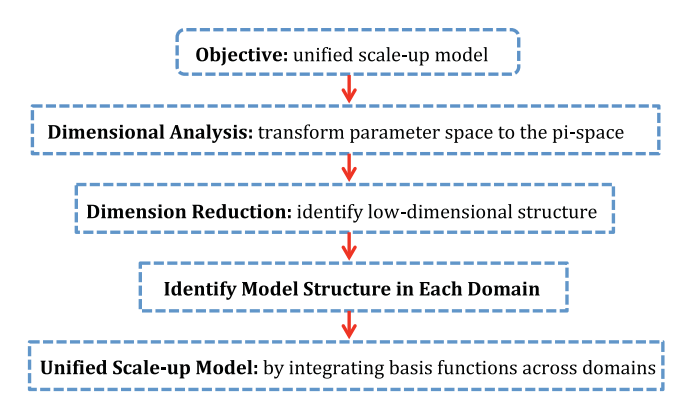


**Figure 1.** Methodology to construct the scale-up model for a multivariate physical system.

structure that only depends on the primary factor, termed as a basis function. Basis functions are assumed to be linearly independent.

The rationale of this definition is based on the observation that physical domains of engineering systems are often classified by one or only a very few dimensionless numbers, which form the *primary factor* henceforth. For example, the Reynolds number is widely used to predict flow patterns in the case of a bounding surface. Laminar flow occurs at low Reynolds numbers where viscous forces dominate, and turbulent flow occurs at high Reynolds numbers where the flow is dominated by inertial forces (Schlichting et al., 1955). In the case of microfluidic droplet formation, four domains are differentiated by the capillary number defined in Equation (4). Since the multipledomain property of the process is fully captured by the primary factor, the original scale-up modeling problem can be divided into several subproblems in lower-dimensional subspaces. Each physical domain is dominated by one mechanism, and the secondary factor contributes to the weights of each mechanism. For instance, the effect of flow rate ratio on the dimensionless size of droplets appears to be linear across different domains (Garstecki et al., 2006; Xu et al., 2008; Wang, Lu, Xu, and Luo, 2009; Zhang and Wang, 2009; Fu et al., 2010), and can thus be treated as a weighting factor of domains.

Based on this rationale, we are now in the position to formulate the high-dimensional multiple-domain scale-up modeling problem. Let z denote the response of interest, and let  $\mathbf{x}^*$ ,  $\mathbf{x}^\circ$  denote the *Primary Factor (PF)* and the *Secondary Factor (SF)* respectively. In the high-dimensional  $\Pi$ -space, there exists the functional relation in Equation (1), where  $\epsilon$  and  $\theta$  denote the random noise and model parameters respectively:

$$z = \Phi(\mathbf{x}^*, \mathbf{x}^\circ) + \epsilon. \tag{1}$$

Projecting the response surface  $\Phi(\mathbf{x}^*, \mathbf{x}^\circ)$  onto the lowerdimensional space spanned by the PF  $\mathbf{x}^*$ , we obtain  $\Phi(\mathbf{x}^*|\mathbf{x}^\circ)$ , i.e., the response conditioning on given settings of the SF  $\mathbf{x}^\circ$ . Since the model structure of  $\Phi(\mathbf{x}^*|\mathbf{x}^\circ)$  in each domain is dictated by  $\mathbf{x}^*$  only, we adopt a set of *linearly independent* basis functions  $S = \{f_i(\mathbf{x}^*)\}_{i=1}^K$  to represent the conditional response function  $\Phi(\mathbf{x}^*|\mathbf{x}^\circ)$  in Equation (2), where  $f_i(\mathbf{x}^*)$  is the *i*th basis function used to characterize a model structure, and its coefficient  $\beta_i$  characterizes the effect of the SF, i.e., a scaling factor for modeling structure  $f_i(\mathbf{x}^*)$ . Note the definition of PF and SF guarantees the existence of model decomposition in Equation (2):

$$\Phi(\mathbf{x}^*|\mathbf{x}^\circ) = \sum_{i=1}^K \beta_i f_i(\mathbf{x}^*), \tag{2}$$

where  $f_i(\mathbf{x}^*)$  is the ith basis function used to characterize a model structure, and its coefficient  $\beta_i$  characterizes the effect of the SF, i.e., a scaling factor for modeling structure  $f_i(\mathbf{x}^*)$ . In the dripping domain with high capillary number, for instance, experimental studies show that droplet size is proportional to  $Ca^{-0.25}$  (Van der Zwan  $et\ al.$ , 2009; Fu  $et\ al.$ , 2010), i.e., a candidate basis function in the dripping domain is  $f_i(Ca) = Ca^{-0.25}$ . It is important to note that the basis functions may vary across domains.

Based on the conditional response model in Equation (2), we deduce the full model in Equation (3). Since the measured response is finite, there exists a reference frame such that the response is always non-negative, and Tonelli's theorem holds. The exchange between sum and integration is thus valid:

$$\Phi(\mathbf{x}^*, \mathbf{x}^\circ; \boldsymbol{\theta}) = \int_{\mathbf{x}^\circ} \Phi(\mathbf{x}^* | \mathbf{x}^\circ) d\mathbf{x}^\circ = \int_{\mathbf{x}^\circ} \sum_{i=1}^K \beta_i(\mathbf{x}^\circ) f_i(\mathbf{x}^*) d\mathbf{x}^\circ$$

$$= \sum_{i=1}^K \left( \int_{\mathbf{x}^\circ} \beta_i(\mathbf{x}^\circ) d\mathbf{x}^\circ \right) f_i(\mathbf{x}^*)$$

$$= \sum_{i=1}^K g_i(\mathbf{x}^\circ) f_i(\mathbf{x}^*), \tag{3}$$

where  $g_i(\mathbf{x}^{\circ})$  can be interpreted as a weight function for  $f_i(\mathbf{x}^*)$  given the settings of the SF  $\mathbf{x}^{\circ}$ , noting that  $g_i(\mathbf{x}^{\circ})'s$  share the function form with different parameters.

Remark 1: The model formulation (3) essentially suggests the statistical additive model framework (Friedman and Stuetzle, 1981; Buja et al., 1989; Hastie and Tibshirani, 1990) for the high-dimensional multiple-domain scale-up modeling problem. The formulation enables the application of modeling techniques in statistics for model building and estimation.

Although the experimental literature can assist in identifying candidate basis functions, there exist discrepancies, due to incomplete physical understanding and variations in experimental conditions and facilities. Furthermore, disagreement and ambiguity in defining the boundaries of physical domains increase the complexity of model building. To accommodate these uncertainties, we will investigate the following framework.

Assumption 1. Let  $\mathbb{S}_d$  denote the subset of basis functions characterizing the model structure of  $\Phi(\mathbf{x}^* \mid \mathbf{x}^\circ)$  in the dth domain,  $d = 1, 2, \ldots, D$ . We assume  $\mathbb{S}_d = \mathbb{S}$  for all d.

Under this framework, the equality  $f_i(\mathbf{x}^*) = 0$  holds only for countable settings of  $\mathbf{x}^*$ . Thus, the basis functions of  $\Phi(\mathbf{x}^* \mid \mathbf{x}^\circ)$  do not degenerate in any continuous domain. Physically, the assumption means that all physical mechanisms, which are characterized by the complete set of basis functions, co-exist in all physical domains with different weights.

Remark 2. Note that the setup of this framework is able to avoid the issue of defining the transition points or boundaries

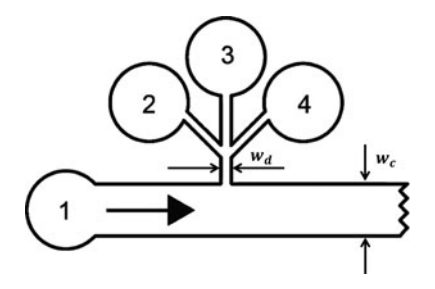


Figure 2. Structure of the two-phase microfluidic T-junction (Lazarus et al., 2012).

between different physical domains upfront. However, implicitly the model  $\Phi(\mathbf{x}^*, \mathbf{x}^\circ)$  selects proper basis function(s) to characterize different physical domains by varying the weight  $g_i(\mathbf{x}^\circ)$  for each basis function  $f_i(\mathbf{x}^*)$ . The influence of a particular mechanism is described by some subset of  $\{g_i(\mathbf{x}^\circ)f_i(\mathbf{x}^*), i=1,\ldots,K\}$ . It follows that both domains and domain transitions can be obtained from the model  $\Phi(\mathbf{x}^*, \mathbf{x}^\circ; \boldsymbol{\theta})$ : (i) a domain is identified to be dominated by a certain mechanism if this mechanism contributes to the majority of response in this domain; (ii) if none of the mechanisms contributes to the majority of response in certain domain, this domain is a transitional domain.

### 3. Scale-up modeling of droplet formation in a coated microfluidic T-junction

This section presents the detailed solution procedure for the high-dimensional scale-up modeling problem formulated in Section 2.

### 3.1. Dimensional analysis and dimension reduction

Before conducting dimensional analysis to obtain the transformed  $\Pi$ -space, we first introduce the droplet formation process in a microfluidic T-junction to identify relevant physical quantities in the parameter space. As shown in Figure 2, the carrier oil (continuous phase) is injected via inlet 1, with the reagent streams being introduced via inlets 2 and 4. A stream injected via inlet 3 is used to prevent diffusive mixing between reagent streams before droplet formation. The immiscible fluid of droplets is called the "dispersed phase."

Notations of physical quantities used in the rest of this article are listed in Table 1.

The parameter space consists of parameters that characterize the geometric structure, properties of the materials and mechanical control variables, which are listed in the relevance list (Table 2). Dimensional analysis is then conducted to generate dimensionless  $\pi$  numbers in Equation (4) that span the

Table 1. Notation.

Notation	Physical quantity			
$\begin{array}{l} w_{c}(w_{d}) \\ h \\ \mu_{c}(\mu_{d}) \\ \rho_{c}(\rho_{d}) \\ Q_{c}(Q_{d}) \\ \sigma \end{array}$	width of channel into which continuous (dispersed) phase flows depth of channel dynamic viscosity of continuous (dispersed) phase density of continuous (dispersed) phase volumetric flow rate of continuous (dispersed) phase interfacial tension			



Table 2. Relevant list of physical quantities.

	Quantity	Dimension
Geometry	$egin{array}{c} w_{ extit{c'}}  w_{ extit{d}} \ h \end{array}$	L
Material	$\mu_c$ , $\mu_d$	$ML^{-1}T^{-1}$ $ML^{-3}$
Mechanics	$Q_{c'}^{\rho_{c'}, \rho_{d}}$ $Q_{c'}^{\rho_{d}}$ $Q_{c'}^{\rho_{d}}$	L <sup>3</sup> T <sup>-1</sup> MT <sup>-2</sup>

transformed  $\Pi$ -space (Garstecki *et al.*, 2006; De Menech *et al.*, 2008; Glawdel and Ren, 2012).

$$\pi_{0} = \bar{L} = \frac{L}{w_{c}}, \quad \pi_{1} = Ca = \frac{\mu_{c}Q_{c}}{\sigma w_{c}h}, \quad \pi_{2} = \lambda = \frac{\mu_{d}}{\mu_{c}}, 
\pi_{3} = Q = \frac{Q_{d}}{Q_{c}}, \quad \pi_{4} = W_{w} = \frac{w_{d}}{w_{c}}, \quad \pi_{5} = W_{h} = \frac{h}{w_{c}}, 
\pi_{6} = \rho = \frac{\rho_{d}}{\rho_{c}}, \quad \pi_{7} = Re = \frac{\rho_{c}Q_{c}}{\mu_{c}w_{c}}.$$
(4)

Corresponding to the formulation in Section 2, we choose the response to be the dimensionless droplet length  $z=\pi_0=\bar{L}$  due to our interest in droplet size. The scale-up modeling problem in the transformed  $\Pi$ -space is then formulated by the  $\pi$  numbers in the form  $\pi_0=\Phi(\pi_1,\pi_2,\pi_3,\pi_4,\pi_5,\pi_6,\pi_7)$ , i.e.,  $\bar{L}=\Phi(Ca,\lambda,Q,W_w,W_h,Re,\rho)$ , with  $(\mathbf{x}^*,\mathbf{x}^\circ)=(Ca,\lambda,Q,W_w,W_h,Re,\rho)$ .

To reduce dimensionality, the capillary number is selected as the primary factor, i.e.,  $x^* = Ca$ , whereas the remaining dimensionless numbers are identified as the SF, which will be explained in Section 3.3. For typical microchannel flows, the Reynolds number Re is very small. Once the microfluidic T-junction design and fluidic materials are determined, the only remaining controllable dimensionless number other than Ca is the flow rate ratio, the effect of which is investigated in each domain. We also qualitatively investigate the effect of  $W_h$  by comparing droplet formation in a microfluidic T-junction with  $W_h = 1$ and  $W_h = 2$ . Therefore, Q and  $W_h$  form the two-dimensional SF  $\mathbf{x}^{\circ} = (Q, W_h)$ . Despite the demonstration in the study of droplet formation in a coated microfluidic T-junction, the strategy to reduce the dimension of a high-dimensional scale-up problem by identifying low-dimensional structures can be applied to a generic high-dimensional scale-up problem.

### 3.2. Experimental setup and data collection

In order to systematically characterize droplet formation across multiple domains, we first select a reference geometry and keep the fluid pair fixed. We used two geometries that maintained a  $w_d: w_c$  ratio of 1:4, with  $w_c=200$  or 400  $\mu$ m. Microfluidic devices were coated with a low-surface-energy fluoropolymer coating using initated chemical vapor deposition as described previously (Lazarus *et al.*, 2012; Riche *et al.*, 2014). The continuous phase was a polychlorotrifluoroethene oil (trade name/vendor: Halocarbon oil), with  $\mu_c=100$  mPa · s and the dispersed phase was de-ionized water. Dimensional parameters for the reference system are given in Table 3. The width ratio  $W_w$  was set to be 0.25, while the depth width ratio  $W_h=1,2$ .

Table 3. Experimental settings of physical quantities.

Fluid System Continuous phase Dispersed phase	Halocarbon oil De-ionized water	Viscosity (mPa · s) 100 1
Device geometry Channel width Channel depth Flow rate control Continuous phase	$egin{array}{c} w_c \ w_d \ h \ Q_c \end{array}$	Dimension (μm) 200–400 50–100 400 Dimension μl/h 250–200 000
Continuous phase Dispersed phase	$Q_c \ Q_d$	250–200 000 12.5–200 000

Droplet length was measured as a function of capillary number Ca and flow rate ratio Q for the reference system by selecting five different flow rate ratios Q = 0.05, 0.25, 0.5, 1, 2. For each fixed flow rate ratio, the capillary number was varied from Ca = 0.00193 to 0.15432. To keep the flow rate ratio fixed, both  $Q_c$  and  $Q_d$  must vary as Ca varies.

As reported in Riche *et al.* (2014), for Ca < 0.05 with  $w_c = 200 \ \mu m$  or Ca < 0.01 with  $w_c = 400 \ \mu m$  respectively, droplet size increased with increasing flow rate ratio at each fixed capillary number explored in the experiment and decreased with increasing Ca at each fixed flow rate ratio (see Figure 3). Unlike droplet formation in uncoated microfluidic channels, droplet formation in the coated device remained in the dripping regime above the threshold of Q = 0.05, and the droplet size appeared to either plateau or increase based on the different flow rate ratio.

### 3.3. Model structures and basis functions

Candidate basis functions that characterize model structures for droplet formation in uncoated microfluidic T-junction in each domain can be acquired from the experimental literature. In squeezing domain ( $Ca \lesssim 0.01$  according to De Menech *et al.* (2008), Ca < 0.002 in Xu *et al.* (2008)), the scaling law is given in the form  $\bar{L} = \sigma + \omega Q$  (Gupta and Kumar, 2010), where  $\sigma$  and  $\omega$  are parameters determined by channel geometry. In the

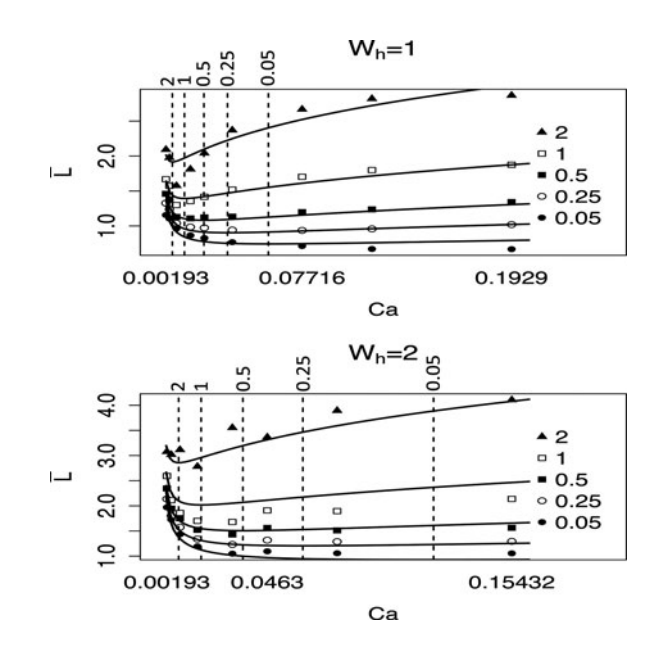


**Figure 3.** Change in dimensionless droplet length  $\bar{L}$  with respect to the capillary number Ca, flow rate ratio Q (from 0.05 to 2) and depth width ratio  $W_h$ .



dripping domain with high Ca where droplets are unconfined, the dimensionless droplet length is approximately proportional to  $Ca^{-0.25}$  (Van der Graaf et~al., 2006; Fu et~al., 2010). In the squeezing-to-dripping domain, according to the correlations discussed in existing studies (Christopher et~al., 2008; Xu et~al., 2008; Wang, Lu, Xu, and Luo, 2009; Zhang and Wang, 2009; Fu et~al., 2010), the scale-up model regarding the capillary number with all the other dimensionless numbers fixed is either given in the general form  $\bar{L}(Ca) \propto Ca^{-\alpha}$  with  $0 < \alpha < 0.25$  or by the dimensionless droplet volume  $\bar{V}(Ca)$  that is a linear combination of  $Ca^{-\alpha_1}$  and  $Ca^{-\alpha_2}$  based on approximation models. According to Assumption 1 in Section 2, droplet formation in the squeezing-to-dripping domain exhibits an intermediate phenomenon. This explains why  $\bar{L}(Ca) \propto Ca^{-\alpha}$  with  $0 < \alpha < 0.25$  in the squeezing-to-dripping domain.

We therefore choose the basis functions  $f_1(Ca) = 1$ ,  $f_2(Ca) = Ca^{-\alpha}$  to characterize the decrease in droplet size in the squeezing and dripping domain, respectively, at relatively low capillary numbers, where  $\alpha$  is a positive parameter to be determined for coated devices.

In addition to the decrease in droplet size as the capillary number increases at relatively low Ca, we observed either a plateau or an increase in droplet size at higher capillary numbers before jetting occurred. We attribute this to the difference between our system and most in the literature using Polydimethylsiloxane (PDMS) channels. The water contact angle of PDMS channels is  $112^{\circ}$  while the low surface energy coating applied to our system renders the channels more hydrophobic, resulting a water contact angle larger than  $120^{\circ}$  (Riche *et al.*, 2014). Wall effects created by coating become significant when the droplet length is larger than the channel geometry. Therefore, an additional basis function  $f_3(Ca) = Ca^{\gamma}$  is proposed to characterize the increase in droplet size at higher capillary numbers with  $\gamma > 0$ . The total number of basis functions is K = 3.

In addition to the PF  $x^* = Ca$ , two SFs  $\mathbf{x} = (Q, W_h)$  are considered to explore the form of  $g_i(\mathbf{x})$  in Equation (3). From observation and existing literature, it is known that: (i) the droplet size is linear with the flow rate ratio with remaining  $\pi$  numbers fixed at high viscosity contrast (Garstecki *et al.*, 2006; Xu *et al.*, 2008; Wang, Lu, Xu, and Luo, 2009; Zhang and Wang, 2009; Fu *et al.*, 2010); (ii) droplet formation with regard to Ca does not depend on the geometry of microfluidic T-junction in squeezing (Gupta and Kumar, 2010), squeezing-to-dripping (Christopher *et al.*, 2008) and in dripping domain (Fu *et al.*, 2010), indicating the independence of  $\alpha$  and  $\gamma$  in  $W_h$ . The weight function  $g_i(Q, W_h)$  is proposed to be

$$g_i(Q, W_h) = \beta_{i,0}(W_h) + \beta_{i,1}(W_h)Q,$$
 (5)

where the intercept and slope of the linear model  $\beta_{i,0}$ ,  $\beta_{i,1}$  are functions of the other SF  $W_h$ .

We analyze the effect of  $W_h$  qualitatively by regarding it as a treatment factor due to the following reasons: (i) the effect of geometry has not been well investigated across domains, i.e., concrete forms of  $\beta_{i0}$  and  $\beta_{i1}$  are not available for some i; (ii)  $W_h$  is a two-level factor in our experiments, which can be represented by  $j = W_h$  with j = 1, 2. Similar to Rogosa (1980), an equivalent expression of Equation (5) can be given in Equation (6), using a dummy variable T defined such that T = 0 for j = 1

Table 4. Reduced model estimation.

Parameter	Estimate	Std.error	P-value
α	0.399 53	0.040 79	3.12e-15
γ	0.245 03	0.017 58	< 2e-16
$\eta_2$	0.090 94	0.025 96	0.000764
$\tau_2$	0.059 91	0.015 21	0.000 177
	0.838 29	0.111 87	8.94e-11
$egin{array}{c} \eta_3 \ eta_3 \end{array}$	1.706 21	0.112 52	< 2e-16
$w_3$	0.846 82	0.087 89	6.36e-15

and T = 1 for j = 2:

$$g_i(T, Q) = \eta_i + \tau_i T + \beta_i Q + w_i T Q, \quad i = 1, ..., K.$$
 (6)

Remark 3: This is essentially an ANCOVA (Analysis of Covariance) model setup in statistical design of experiments, which is a generalized linear model blending ANOVA (Analysis of Variance) with regression.  $g_i(T,Q)$  is the response for a given value of covariate Q and a selection of treatment T,  $\tau_i$  refers to the difference in  $\beta_{i,0}(W_h)$  due to the treatment effect,  $\beta_i$  is the regression coefficient for the covariate Q, and  $w_i$  is the contrast in  $\beta_{i,1}(W_h)$  due to an interaction between the treatment factor T and the covariate Q.

Based on Assumption 1 and the discussions above, the basis functions of  $\Phi(Ca|Q)$  are obtained as  $\mathbb{S} = \{1, Ca^{-\alpha}, Ca^{\gamma}\}$ . According to Equation (6), the unified scale-up model under the assumption is given in the form of Equation (7), with K = 3 and T = 0, 1 denoting  $W_h = 1$ , 2, respectively:

$$\Phi(Ca, Q, T) = \sum_{i=1}^{K} \{ \eta_i + \tau_i T + \beta_i Q + w_i T Q \} f_i(Ca).$$
 (7)

### 3.4. Model estimation

The nls() function in the R language was applied for Nonlinear Least Squares estimation (Fox and Weisberg, 2010), using a form of Gauss–Newton iteration that employs numerically approximated derivatives. The full model in Equation (7) is further reduced to the model in Equation (8) by eliminating redundant terms to minimize the residual standard error, estimation given in Table 4.

$$\Phi(Ca, Q, T) = (\eta_2 + \tau_2 T)Ca^{-\alpha} + [\eta_3 + \beta_3 Q + w_3 TQ]Ca^{\gamma}$$
(8)

### 4. Discussions

### 4.1. Physical insights obtained through high-dimensional modeling

Compared with the one-factor-at-a-time approach, our generic methodology allows investigation into the overall model structure in the high-dimensional space, providing additional insights into the droplet formation process in coated microfluidic devices:

1. Flexibility for full-scale production

As observed from Figure 3, the concise model in Equation (8) captures well the influence of Ca, Q, and  $W_h$  simultaneously, providing an opportunity to optimize multiple parameters simultaneously for full-scale production.

### 2. Interpretation of multiple physical domains

Domains are identified by dominant physical mechanisms characterized by corresponding basis functions. As observed from Equation (8), a dripping mechanism characterized by  $f_2(Ca)$  dominates the decrease in droplet size before  $f_3(Ca)$  starts to dominate the increase in droplet size. The transition between domains depends on the SF.

### 3. Effect of coating

Coating enables a wider range of producing stable droplets, allowing higher flow rate ratios and capillary numbers. Although physical domains can still be classified based on different dominant mechanisms characterized by corresponding basis functions of the capillary numbers, the range of each physical domain could be very different from that of droplet formation in uncoated microfluidic devices, e.g., squeezing mechanism characterized by  $f_1(Ca)$  is not significant within our explored range, whereas in a coated T-junction, squeezing dominates droplet formation for Ca < 0.002 and is competitive with dripping mechanism for 0.002 < Ca < 0.01.

### 4. Effect of SF

Transitions between physical domains are not independent of the SF (Q,  $W_h$  discussed in our case). This will be further explained in the discussion of identifying physical domains.

### 4.2. Identification of physical domains and boundaries

The scale-up model in Equation (8) not only provides some insights into the droplet formation process in a coated microfluidic T-junction, but also demonstrates the possibilities of detecting physical domains dominated by different mechanisms without ambiguity in boundaries that are characterized by values of the PF in the literature. Physical domains in this scale-up droplet formation process are detected by identifying dominant mechanisms:

### 1. Identification of relevant mechanisms

As observed in model reduction from Equation (7) to (8),  $f_1(Ca)$  is eliminated from the final model, as it is not significant across investigated domains. This implies that the squeezing mechanism characterized by  $f_1(Ca)$  in our coated devices is not significant within the explored range, i.e., coating leads to a decrease in the lower bound of the dripping domain with respect to the primary factor Ca as a benefit of low surface energy.

Remark 4: As observed from Figure 3, there exists a slight lack of fit under  $W_h = 2$ . This can be attributed to the inconspicuous postponement of the dripping domain compared with the case when  $W_h = 1$ . In other words, when  $W_h = 2$ , droplet formation near the lower bound of explored Ca may actually fall in to the squeezing-to-dripping domain, although the basis function  $f_1(Ca)$  is still recognized as insignificant, due to the narrow range of the squeezing-to-dripping domain even if it exists.

## 2. Identification of dominant mechanisms The dripping mechanism characterized by $f_2(Ca)$ dominates the decrease of droplet size at low capillary

**Table 5.**  $Ca_1(Q, T)$ .

		Q				
	0.05	0.25	0.5	1	2	
T = 0 T = 1	0.0055 0.0071	0.012 0.017	0.023 0.036	0.036 0.062	0.059 0.12	

**Table 6.**  $Ca_{2}(Q, T)$ .

	Q				
	0.05	0.25	0.5	1	2
T = 0 $T = 1$	0.014 0.019	0.032 0.044	0.060 0.093	0.094 0.16	0.15 0.31

numbers within our explored range, whereas the droplet size starts to increase and then tends to reach a plateau as Ca increases to a certain level. The domain in which the size of stable droplets increases is identified as the "dripping-to-jetting" domain, due to the coexistence of partial characteristics: (i) stable droplets are produced in this domain with no observations of jets; (ii) droplet size tends to reach a plateau near the explored upper bound of Ca, consistent with the scale-up model in the jetting domain Fu et al. (2012) which merely depends on Ca.

### 3. Identification of boundaries

Noting that  $f_2(Ca) = Ca^{\alpha}$  and  $f_3(Ca) = Ca^{\gamma}$  are both monotonic with respect to Ca, a transition point between dripping and dripping-to-jetting domains can be defined as the solution to  $\partial \Phi(Ca, Q, T)/\partial Ca = 0$  given in Equation (9):

$$Ca_1(Q, T) = \left[ \frac{\alpha(\eta_2 + \tau_2 T)}{\gamma[\eta_3 + (\beta_3 + w_3 T)Q]} \right]^{\frac{1}{\alpha + \gamma}}.$$
 (9)

When  $Ca < Ca_1(Q, T)$ , the droplet size decreases, i.e., the dripping mechanism depicted by  $Ca^{-\alpha}$  explains a larger portion of the change in droplet size; when  $Ca > Ca_1(Q, T)$ , the droplet size starts to increase, i.e., dripping-to-jetting mechanism depicted by  $Ca^{\beta}$  contributes to a larger percentage of size change.

As shown in Table 5 and Figure 3 (dashed lines), the value of  $Ca_1(Q, T)$  is smaller at higher flow rate ratio Q, and the transition is postponed due to extra confinement with  $W_h = 2$  (T = 1) compared with the case with  $W_h = 1$  (T = 0).

### 4. Effect of secondary factor

To further demonstrate the effect of the SF on boundaries between physical domains, we define  $Ca_2(Q, T)$  as the solution to  $\partial^2 \Phi(Ca, Q, T)/\partial Ca^2 = 0$  given in Equation (10) and Table 6, noting that  $Ca_2(Q, T) > Ca_1(Q, T)$ :

$$Ca_{2}(Q,T) = \left[\frac{\alpha(1+\alpha)(\eta_{2}+\tau_{2}T)}{\gamma(1-\gamma)[\eta_{3}+(\beta_{3}+w_{3}T)Q]}\right]^{\frac{1}{\alpha+\gamma}}.$$
(10)

In the dripping domain with  $Ca < Ca_1(Q, T) < Ca_2(Q, T)$ ,  $\partial^2 \Phi(Ca, Q, T)/\partial Ca^2$  is positive with  $Ca_2(Q, T)$  decreasing in Q, which explains the sharper decrease at lower Q when Ca is close to the lower bound of the explored range. In the dripping-to-jetting



domain with  $Ca > Ca_1(Q, T)$ , the increase in droplet size with respect to Ca first accelerates in the range of  $Ca < Ca_2(Q, T)$  and then decelerates to reach a plateau at higher  $Ca > Ca_2(Q, T)$ .

### 5. Conclusions

We formulated a generic multiple-domain scale-up problem and proposed a scalable modeling approach to predict manufacturing processes that can potentially operate under multiple physical domains due to uncertainties. The approach addresses two critical challenges in scale-up modeling for multiple-domain manufacturing processes: high dimensionality and multiple physical domains. The challenge of high dimensionality is addressed by identifying low-dimensional model structures through dimensional analysis and adoption of the PF. The ambiguity in boundaries between physical domains is addressed by interpreting multiple-domain manufacturing processes as an outcome of coexisting mechanisms. Physical domains are identified by identifying dominant mechanisms.

The proposed formulation and approach have been applied and demonstrated to investigate the scale-up droplet formation process in coated microfluidic T-junction. The unified scale-up model across multiple domains not only closely captures the joint effect of capillary number, flow rate ratio, and depth width ratio, but also leads to some physical insights into the process: (i) droplet formation in the coated device can be explained by coexisting mechanisms with weights varying across domains; (ii) variables in addition the capillary number influence the transition from dripping to dripping-to-jetting domain, which is postponed at lower flow rate ratio and higher depth width ratio; (iii) the low-surface-energy fluoropolymer coating has proved to significantly extend the range of domain for producing stable droplets either in dripping or dripping-to-jetting domain.

### **Funding**

Huang's work is supported by National Science Foundation (NSF) with CAREER grant number CMMI-1055394. Malmstadt's work is supported by NSF grant CMMI-1068212.

### **Notes on contributors**

*Yanqing Duanmu* received her B.S. in physics from the University of Science and Technology of China in 2012. She earned her Ph.D. degree in industrial and systems engineering and an M.S. in statistics from the University of Southern California in 2017 under the guidance of Professor Qiang Huang. She is a member of INFORMS. Currently, she is a senior analyst for statistics and operations research at United Airlines.

Carson T. Riche received his B.S. in chemical and biomolecular engineering from Johns Hopkins University in 2010. He earned his Ph.D. from the University of Southern California in chemical engineering in 2015 under the guidance of Professors Noah Malmstadt and Malancha Gupta. He was a postdoctoral scholar in the lab of Professor Dino Di Carlo at the University of California, Los Angeles. Currently, he is an R&D Engineer at Labcyte Inc.

*Malancha Gupta* is the Jack Munushian Early Career Chair Associate Professor in the Mork Family Department of Chemical Engineering and Materials Science at the University of Southern California. She received her B.S. in chemical engineering from the Cooper Union in 2002. She received her

Ph.D. in chemical engineering from the Massachusetts Institute of Technology in 2007 under the guidance of Professor Karen Gleason. From 2007-2009, she was a postdoctoral fellow in the Department of Chemistry and Chemical Biology at Harvard University working under the guidance of Professor George Whitesides. She has received several awards including the ACS PRF Doctoral New Investigator Award in 2012, the NSF CAREER Award in 2013, and the USC Viterbi School of Engineering Junior Faculty Research Award in 2014.

Noah Malmstadt is an associate professor at the University of Southern California. He received a B.S. in chemical engineering from Caltech and a Ph.D. in bioengineering from the University of Washington. Following postdoctoral work at UCLA, he joined the Mork Family Department of Chemical Engineering and Materials Science at USC in 2007. He is the recipient of a 2012 Office of Naval Research Young Investigator award and is a 2017 Association of Laboratory Automation JALA 10 Honoree. His research focuses on microfluidic strategies to facilitate material fabrication and biophysical analysis. He has pioneered the integration of ionic liquids as solvents in droplet microreactors and the application of microfluidic systems to synthesizing biomimetic cell membranes. Microfluidic analytical techniques he has developed include methods for measuring the permeability of cell membranes to druglike molecules and techniques for measuring ionic currents through membrane proteins.

Qiang Huang received his Ph.D. degree in industrial and operations engineering from the University of Michigan-Ann Arbor. He is currently an associate professor at the Daniel J. Epstein Department of Industrial and Systems Engineering, University of Southern California (USC), Los Angeles. He was the holder of Gordon S. Marshall Early Career Chair in Engineering at USC from 2012 to 2016. He received a National Science Foundation CAREER award in 2011 and IEEE Transactions on Automation Science and Engineering Best Paper Award from IEEE Robotics and Automation Society in 2014. He is department editor for IISE Transactions, associate editor for ASME Transactions, Journal of Manufacturing Science and Engineering, and a member of the editorial board for Journal of Quality Technology. He also served an associate editor for IEEE Transactions on Automation Science and Engineering and for IEEE Robotics and Automation Letters. He is a senior member of IEEE and a member of INFORMS, ASME and IISE.

### References

Anna, S.L., Bontoux, N. and Stone, H.A. (2003) Formation of dispersions using flow focusing in microchannels. *Applied Physics Letters*, **82**(3), 364–366.

Barenblatt, G.I. (2003) Scaling, vol. 34, Cambridge University Press, Cambridge, UK.

Buja, A., Hastie, T. and Tibshirani, R. (1989) Linear smoothers and additive models. *The Annals of Statistics*, 17(2), 453–510.

Christopher, G.F. and Anna, S.L. (2007) Microfluidic methods for generating continuous droplet streams. *Journal of Physics D: Applied Physics*, 40(19), R319.

Christopher, G.F., Noharuddin, N.N., Taylor, J.A. and Anna, S.L. (2008) Experimental observations of the squeezing-to-dripping transition in t-shaped microfluidic junctions. *Physical Review.E, Statistical, Nonlinear, and Soft Matter Physics*, **78**(3), 036317-1–036317-12.

Demello, A.J. (2006) Control and detection of chemical reactions in microfluidic systems. *Nature*, 442(7101), 394–402.

De Menech, M., Garstecki, P., Jousse, F. and Stone, H.A. (2008) Transition from squeezing to dripping in a microfluidic t-shaped junction. *Journal of Fluid Mechanics*, **595**, 141–161.

Fox, J. and Weisberg, S. (2010) An R Companion to Applied Regression. Sage, Thousand Oaks, CA.

Friedman, J.H. and Stuetzle, W. (1981) Projection pursuit regression. *Journal of the American Statistical Association*, **76**(376), 817–823.

Fu, T., Ma, Y., Funfschilling, D. and Li, H.Z. (2009) Bubble formation and breakup mechanism in a microfluidic flow-focusing device. *Chemical Engineering Science*, 64(10), 2392–2400.

Fu, T., Ma, Y., Funfschilling, D., Zhu, C. and Li, H.Z. (2010) Squeezing-to-dripping transition for bubble formation in a microfluidic t-junction. *Chemical Engineering Science*, **65**(12), 3739–3748.



- Fu, T., Wu, Y., Ma, Y. and Li, H.Z. (2012) Droplet formation and breakup dynamics in microfluidic flow-focusing devices: From dripping to jetting. *Chemical Engineering Science*, 84, 207–217.
- Garstecki, P., Fuerstman, M.J., Stone, H.A. and Whitesides, G.M. (2006) Formation of droplets and bubbles in a microfluidic t-junction-scaling and mechanism of break-up. *Lab on a Chip*, **6**(3), 437–446.
- Glawdel, T. and Ren, C.L. (2012) Droplet formation in microfluidic t-junction generators operating in the transitional regime. iii. dynamic surfactant effects. *Physical review E, Statistical, Nonlinear, and Soft Matter Physics*, **86**(2), 026308-1–026308-12.
- Gupta, A. and Kumar, R. (2010) Effect of geometry on droplet formation in the squeezing regime in a microfluidic t-junction. *Microfluidics and Nanofluidics*, **8**(6), 799–812.
- Hastie, T.J. and Tibshirani, R.J. (1990) Generalized additive models, volume 43 of Monographs on Statistics and Applied Probability. Chapman and Hall, Boca Raton, FL.
- Huang, Q., Wang, L., Dasgupta, T., Zhu, L., Sekhar, P.K., Bhansali, S. and An, Y. (2011) Statistical weight kinetics modeling and estimation for silica nanowire growth catalyzed by Pd thin film. *IEEE Transactions on Automation Science and Engineering*, 8(2), 303–310.
- Lazarus, L.L., Riche, C.T., Marin, B.C., Gupta, M., Malmstadt, N. and Brutchey, R.L. (2012) Two-phase microfluidic droplet flows of ionic liquids for the synthesis of gold and silver nanoparticles. ACS Applied Materials & Interfaces, 4(6), 3077–3083.
- Link, D., Anna, S.L., Weitz, D. and Stone, H. (2004) Geometrically mediated breakup of drops in microfluidic devices. *Physical Review Letters*, **92**(5), 054503-1–054503-4.
- Riche, C.T., Zhang, C., Gupta, M. and Malmstadt, N. (2014) Fluoropolymer surface coatings to control droplets in microfluidic devices. *Lab on a chip*, **14**(11), 1834–1841.
- Rogosa, D. (1980) Comparing nonparallel regression lines. *Psychological Bulletin*, **88**(2), 307–321.
- Schlichting, H., Gersten, K., Krause, E., Oertel, H. and Mayes, K. (1955). Boundary-Layer Theory, vol. 7, McGraw-Hill: New York, NY.
- Tan, J., Li, S.W., Wang, K. and Luo, G.S. (2009) Gas-liquid flow in t-junction microfluidic devices with a new perpendicular rupturing flow route. *Chemical Engineering Journal*, 146(3), 428–433.
- Teh, S.-Y., Lin, R., Hung, L.-H. and Lee, A.P. (2008) Droplet microfluidics. *Lab on a chip*, **8**, 198–220.

- Thorsen, T., Roberts, R.W., Arnold, F.H. and Quake, S.R. (2001) Dynamic pattern formation in a vesicle-generating microfluidic device. *Physical Review Letters*, 86(18), 4163–4166.
- van der Graaf, S., Nisisako, T., Schroen, C., van Der Sman, R. and Boom, R. (2006) Lattice Boltzmann simulations of droplet formation in a t-shaped microchannel. *Langmuir*, **22**(9), 4144–4152.
- Van der Zwan, E., van der Sman, R., Schroën, K. and Boom, R. (2009) Lattice Boltzmann simulations of droplet formation during microchannel emulsification. *Journal of Colloid and Interface Science*, 335(1), 112–122.
- Wang, K., Lu, Y.C., Xu, J.H. and Luo, G.S. (2009) Determination of dynamic interfacial tension and its effect on droplet formation in the t-shaped microdispersion process. *Langmuir*, 25(4), 2153–2158.
- Wang, L. and Huang, Q. (2013) Cross-domain model building and validation (CDMV): A new modeling strategy to reinforce understanding of nanomanufacturing processes. *IEEE Transactions on Automation Science and Engineering*, 10(3), 571–578.
- Wang, S.S., Jiao, Z.J., Huang, X.Y., Yang, C. and Nguyen, N.T. (2009) Acoustically induced bubbles in a microfluidic channel for mixing enhancement. *Microfluidics and Nanofluidics*, 6(6), 847–852.
- Xu, J.H., Li, S.W., Tan, J. and Luo, G.S. (2008) Correlations of droplet formation in t-junction microfluidic devices: from squeezing to dripping. *Microfluidics and Nanofluidics*, 5(6), 711–717.
- Xu, L., Wang, L. and Huang, Q. (2015) Growth process modeling of semiconductor nanowires for scale-up of nanomanufacturing: A review. IIE Transactions, 47(3), 274–284.
- Xu, Q., Hashimoto, M., Dang, T.T., Hoare, T., Kohane, D.S., Whitesides, G.M., Langer, R. and Anderson, D.G. (2009) Preparation of monodisperse biodegradable polymer microparticles using a microfluidic flowfocusing device for controlled drug delivery. Small (Weinheim an der Bergstrasse, Germany), 5(13), 1575–1581.
- Zhang, Y. and Wang, L. (2009) Experimental investigation of bubble formation in a microfluidic t-shaped junction. Nanoscale and Microscale Thermophysical Engineering, 13(4), 228–242.
- Zhao, C.-X. and Middelberg, A.P.J. (2011) Two-phase microfluidic flows. Chemical Engineering Science, 66(7), 1394–1411.
- Zlokarnik, M. (1991) Scale-up in Chemical Engineering. Wiley-VCH Verlag GmbH & Co. KGaA.